

ESTIMATION OF THE SNR FOR WIRELESS SYSTEMS IN A LOCAL FADING ENVIRONMENT WITH MULTI-ELEMENT ANTENNAS

Jean-Pierre Dubois

Department of Electrical Engineering, University of Balamand
Deir El Balamand, North District, Lebanon
phone: + (961) 3841476, fax: + (961) 6930250, email: jeanpierre_dubois@hotmail.com
web: www.balamand.edu.lb

ABSTRACT

Estimation techniques for the signal-to-noise ratio play an increasingly vital role in the effective operation of wireless communication systems. This paper presents stochastic models and estimation algorithms for the average received signal-to-interference-noise ratio (SINR) in local fading area channels with a finite random number of scatterers for wireless single-input-single-output (SISO) and multiple-input-multiple-output (MIMO) systems. The stochastic models for the SINR are based on a doubly stochastic filtered compound Poisson point process. For each of these statistical models, we present optimal and computationally efficient estimation algorithms to determine the average SINR using received diffuse power measurements. We show that the maximum likelihood estimator is optimal in the sense that the variance of the error is the smallest possible using any other conceivable estimate having the same bias with the same data. Efficient estimation of the SINR also allows accurate quantification of the bit error rate and average channel capacity for adequate quality of service (QoS) and network link resource allocation.

1. INTRODUCTION

Wireless technology presents engineers with a uniquely different design challenge. Previously, most radio systems operated in a noise-limited radio channel, where thermal receiver noise was the sole dominant source of signal quality degradation. In a wireless environment, the random spatial distribution of diffusing scatterers in the multipath fading channel causes the received signal power to randomly fluctuate, thus rendering the received SNR a random variable [1]. Since the performance of the radio link depends on maintaining an adequate SNR, using various techniques, notably equalization, estimating the SNR is of paramount importance.

Channel capacity is the unifying characteristic of digital communication systems. The success or failure of communications is dictated by the capacity of the link, best measured in terms of bit rate. It is the wireless channel that places the ultimate capacity limitation on the network. Shannon universal formulation for the upper-limit channel capacity C in terms of SINR and transmission bandwidth B assumes that the interference is additive white Gaussian noise [2]:

$$C = B \log_2(1 + \text{SINR}) \text{ bits/s} \quad (1)$$

Although the wireless channel is more complicated than the AWGN channel, there is basic truth that for a given bandwidth, the SINR determines the absolute channel capacity. A randomly fluctuating SINR will clearly cause the channel capacity to fluctuate. Estimating the SINR is of paramount importance in MIMO receiver diversity techniques such as maximum ratio combination (MRC). In addition, through efficient SINR estimation techniques, the average BER and channel capacity can be accurately quantified. This is of crucial importance because if adequate network resources are not allocated and the receiver does not receive enough power, no modulation or equalization technique will produce an acceptable data rate [3].

To quantify the effects of a fading channel on the average SNR, channel capacity, and receiver performance, we must first quantify the statistical distribution of received power that a receiver experiences in a random multipath channel.

2. MODELING OF THE LOCAL FADING CHANNEL

Key to the development of efficient estimation and detection schemes are accurate modelling and in-depth stochastic analysis of wireless

channels. The network structure to support wireless and mobile multimedia and internet communications consists of various components at different scales ranging from mega- (global) and macro- to pico- and as little as femto-cellular sizes. Classically, these channels have been assumed to be fully developed, that is, comprising an infinite number of scatterers, leading to well known multipath fading models such as Rayleigh, Rician, lognormal, and Nakagami- m . These models may work well (but not always) for large cellular structures, mainly, mega-, macro-, and micro-cells which dominate 2G, 2.5G and some 3G systems such as GSM, GPRS, DECT, EDGE and UMTS. With the emerging and planning of new wireless technologies, cell sizes have been reduced to pico- and femto-levels especially for Bluetooth, WiFi, and a multitude of other WLAN, WPAN and wireless ad-hoc networks in the planning [4]. The channel fading models in these small cells, which we term stochastically local area channel (SLAC), would no longer follow classical fully-developed noise models, thus triggering the need to develop newer more accurate stochastic models for fading.

There are also many other propagation scenarios where the received signal comprises a small random number of multipath waves. While this typically occurs for narrowband receiver operation, directional antennas and wideband signals increase the likelihood of *partially developed fading*. In fact, directive antennas or arrays tend to amplify several of the strongest multipath waves arriving in a particular direction while attenuating the remaining waves [5]. Also, wideband receivers have the ability to reject multipath components that arrive with largely different time delays, effectively retaining only a small number of multipath waves [5], which we consider random for more accurate analysis.

2.1 A New Perspective in Fading Analysis

The *old perspective* was to treat multipath fading noise as a nuisance with the ultimate goal of combating the distortion it causes. In this context, modern cellular systems use adaptive equalization to reduce multipath by subtracting the reflected multipath signals from the received signal through the use of digital filters that dynamically change their characteristics in response to different situations [3]. Such techniques are expensive, computationally demanding, and suffer from increased latency (delay) which is clearly undesirable in real-time transmission.

We treat the scattering phenomena from a *new perspective*: as a carrier of useful signal's envelope (and power) information. In our approach, we plan to make use of the fact that multipath fading is a function of the amplitude strength and spatial distribution of scatterers within the channel on a scale corresponding to the wavelength of the transmitted wave. Scattering noise is thus viewed as carrier of information about the envelope and power statistics of multipath waves within a channel. These characteristics are useful in average received power quantification.

In short, our goal is not to combat multipath per se, but rather to use multipath statistical properties advantageously in developing techniques for determining the average received power. We model the scattering channel elements using a random point process whose rate is determined by an underlying *information process*. We then estimate the average received power, and consequently the average received SINR and channel capacity, using diffuse power measurements.

2.2 Doubly Stochastic Filtered Compound Poisson Point Model

One common approach to modeling random scattering is to assume that the backscattered return within a resolution element arises from the collection of elemental point scatterers. The total backscattered field is then taken to be the sum of the scattered fields

from all of the elemental scatterers. The amplitude of the scattered field from each of these elemental scatterers will in general be a function of their size and physical properties. Thus in general, the amplitude of the field scattered by each elemental scatterer can be a random variable.

For most wireless multipath channels, the locations of the elemental scatterers can be viewed as random, and furthermore, the number of elemental scatterers within a channel will be a random variable. One of the most effective methods for modeling "elements" that occur randomly in space is to use a *point process* [6]. If, in addition, there is attached to each point (random location) a random quantity that can be represented by one or more random variables (in this case the amplitude and phase of the backscattered field), the natural stochastic model to use is that of a *marked point process*. Furthermore, for many multipath channels, the number of elemental scatterers in disjoint regions will be statistically independent integer-valued random variables and the point process is termed a *compound point process*. If in addition, the point process satisfies a technical condition called *Khinchine orderliness* then the point process will be a Poisson point process. The number of elemental scatterers within a channel will be a Poisson random variable with intensity or rate λ , which in turn is random. For this reason, a *doubly stochastic compound Poisson point process* is a useful model of random scattering in wireless channels.

When the number of scattering points within a channel is sufficiently large that the central limit theorem (CLT) holds and the scattered field is approximately a circular complex Gaussian random variable, we say that the fading noise is *fully developed*. But if the number of points is relatively small, typically less than 10 to 20 as in a SLAC, the fading noise is not fully developed. In this case, the doubly stochastic compound point process is useful for characterizing the *partially developed fading*, and estimates of the intensity λ can be used to characterize the average received diffuse power. We now investigate the use of doubly stochastic compound point process for this purpose.

2.3 Single-Input-Single-Output Scattering Channel

A multipath channel is assumed to contain a collection of N elemental points representing scatterers randomly distributed throughout the region, with each elementary scatterer amplitude distributed independently of the amplitudes of other scatterers. The random spatial distribution of the scatterers arrivals is described by a point process with a set of points having associated complex marks E_j , ($j = 1, \dots, N$) corresponding to the j -th scatterer. Each mark component E_j has a random amplitude ξ_j corresponding to the energy absorption of the j -th scatterer and a random phase ϕ_j uniformly distributed over the interval $[0, 2\pi)$. We assume that the number of scattering points within a multipath channel is Poisson distributed with intensity λ . The resultant scattered multipath field is the superposition of the multipath waves scattered by elemental scatterers:

$$\kappa_N = \sum_{j=1}^N E_j = \sum_{j=1}^N \xi_j e^{i\phi_j} \quad (2)$$

The resulting process is a *mark-accumulator Poisson point process*, a special type of *filtered compound Poisson point process*, and λ is the intensity of this process. Since λ itself is a random process, the point process described in Eq.(2) is a *doubly stochastic filtered compound Poisson point process* [6]. The power of the received faded signal in a SISO system is obtained by forming the square of the envelope of the total scattered electric field:

$$v_N = \left| \sum_{j=1}^N \xi_j e^{i\phi_j} \right|^2 \quad (3)$$

2.4 Multiple-Input-Multiple-Output Scattering Channel

MIMO systems use multiple antennas at both transmitter and receiver ends for communication [1]. Independent channel fading caused by multipath between transmitting and receiving antennas provides a significant capacity gain and link reliability over conventional single antenna systems. Channels independence also means that the receiver will have more than one independent replica of the transmitted signal.

Diversity schemes are used to generate multiple signal branches between transmitter and receiver [1] and are promising techniques for overcoming multipath fading in a wireless channel without adding inordinate complexity to the receiver unit. For single-input-multiple-output (SIMO) systems with L antennas at the receiver, diversity receivers extract multiple signal branches or copies of the same signal

received from different channels and apply gain combining schemes such as equal gain combining (EGC) to enhance the signal-to-fading-noise ratio and improve the system's performance.

In the multi-diversity model, L -statistically independent diversity measurements are obtained. EGC of the received power of independent signal branches involves the noncoherent sum of L statistically independent single realizations of the mark measurements v_{NL} ($l=1, 2, \dots, L$):

$$\psi_{NL} = \sum_{l=1}^L v_{NL} \quad (4)$$

Although in our analysis we consider SIMO ($1 \times L$) systems, the results can be extended to MIMO ($M \times L$) systems. In fact, using simple *spatial cycling* techniques [7], MIMO systems are implemented by using only one transmitter at a time and by cycling over the M transmitters periodically. A SIMO structure is effectively employed at every transmission period.

2.5 Amplitude Models of Complex Marks

Since the elementary scatterers have varying statistical characteristics, we expect the amplitudes of the complex marks to be governed by different models. We consider 2 models: (1) the amplitudes of the scatterers are fixed, and (2) the amplitudes are Rayleigh distributed.

In the case of Rayleigh distributed amplitudes, we consider the resolution region as made up of a small number of scattering centers (Rayleigh center), with each center made up of a large number of elementary scatterers. This model is especially descriptive of wireless channels in an urban environment with large reflectance amplitudes for the scatterers (such as large buildings) and is a direct result of the central limit theorem. For fully-developed fading, the Nakagami- m model would be the most appropriate under this scenario.

3. ESTIMATION TECHNIQUES

3.1 Constant Amplitude Model

3.1.1 Maximum Likelihood Estimation

The objective is to estimate the rate λ of the Poisson process from the mark measurements given in Eqs. (3) and (4). This estimation problem is rather difficult since the parameter λ to be estimated is implicitly imbedded in the power measurements as the rate λ of the compound Poisson process. Due to the mathematical complexity of the likelihood function for both SISO and multi-diversity cases, we formulate an expectation-maximization (EM) algorithm [6] to produce a recursive maximum likelihood (ML) estimate of λ . We show that the EM algorithm is implemented recursively, starting with an admissible initial estimate $\hat{\lambda}^{[0]} \geq 0$, according to:

$$\hat{\lambda}^{[k+1]} = \begin{cases} A^{-1}, & \psi = L \\ \frac{\phi(\psi, \hat{\lambda}^{[k]})}{Ap_{\lambda}^c(\psi)|_{\lambda=\hat{\lambda}^{[k]}}}, & \psi \neq L \end{cases} \quad (5)$$

$$p_{\lambda}^c(\psi) = e^{-\lambda A} \left(\begin{aligned} & (0.5\lambda A\pi^{-1})^2 K\left(\frac{1}{4}\sqrt{\psi(8-\psi)}\right) I_{[0.4, (4,8)]}(\psi) \delta_{L2} \\ & + \Gamma^{-1}(L) \psi^{L-1} \sum_{n=0}^{n_L} \frac{(\lambda A)^n}{n! n^{L-1}} \exp(-\psi/n) \left(1 + \sum_{m=1}^{M_L} c_m \zeta_m^{L-1}(\psi/n) \right) I_{[0, \infty)}(\psi) \\ & + \Gamma^{-1}(L) \psi^{L-1} \sum_{n=n_L+1}^{\infty} \frac{(\lambda A)^n}{n! n^{L-1}} \exp(-\psi/n) I_{[0, \infty)}(\psi) \end{aligned} \right) \quad (6)$$

$$\phi(\psi, \hat{\lambda}^{[k]}) = e^{-\lambda A} \left(\begin{aligned} & (0.5\lambda A\pi^{-1})^2 K\left(\frac{1}{4}\sqrt{\psi(8-\psi)}\right) I_{[0.4, (4,8)]}(\psi) \delta_{L2} \\ & + \Gamma^{-1}(L) \psi^{L-1} \sum_{n=0}^{n_L} \frac{(\lambda A)^n}{n! n^{L-1}} \exp(-\psi/n) \left(1 + \sum_{m=1}^{M_L} c_m \zeta_m^{L-1}(\psi/n) \right) \\ & + \Gamma^{-1}(L) \psi^{L-1} \sum_{n=n_L+1}^{\infty} \frac{(\lambda A)^n}{n! n^{L-1}} \exp(-\psi/n) I_{[0, \infty)}(\psi) \end{aligned} \right) \quad (7)$$

The functions $\zeta_m^{L-1}(\cdot)$ are the generalized Laguerre polynomials, $K(\cdot)$ is the complete elliptic function, A is a parameter equal to the reciprocal of the mean reflectance strength of the scatterers (mean-square of the amplitudes), and the coefficients c_m are tabulated in [8].

The EM algorithm was numerically implemented for various values of λ (assumed known). The results after k iterations are shown in Figs. 1 and 2 for different numbers of observations. In all cases, the sequence of estimates $\hat{\lambda}^{[k]}$ converges towards the ML estimator.

3.1.2 Performance of the Maximum Likelihood Estimator

The performance of the estimator is characterized by the bias $b(\lambda)$ and by comparing the variance of the error with the Cramer-Rao lower bound (CRLB) defined as [6]:

$$\text{CRLB}(\lambda) = J_L^{-1}(\lambda) \left(1 - \frac{db(\lambda)}{d\lambda} \right)^2 \quad (8)$$

where $J_L(\lambda)$ is the Fisher information matrix.

The expected value of the estimator $E(\hat{\lambda})$ is estimated using Monte Carlo simulation of the marks measurements. The numerical results are illustrated in Fig. 3 for 1 and 2 antennas. We note that the bias is reduced as the number of antennas is increased. This is a direct result from the property that the ML estimator is a consistent estimator.

We can estimate the variance of the estimator and the Cramer-Rao lower bound using Monte Carlo simulation of marks measurements. Figure 4 provides a comparison between the estimated variance of the error and the estimated CRLB as a function of the rate λ , for various number of power measurements. For a given number of observations, the variance of the error and the CRLB increase as the rate gets larger. This follows from the fact that the rate and the variance of the Poisson process are equal. As the rate increases, so does the variance of the Poisson process, causing a lower performance of the estimator. As the number of diversities is increased, the variance of the error and the CRLB decrease, and in addition, the variance of the error gets closer to the CRLB. The fact that the performance of the estimator improves with a larger number of observations is a direct result of the consistency property of the ML estimator.

Overall, it is evident from these published graphs that the performance of the ML estimator is very good. For rates lower than 20, the variance of the error is very close to the CRLB when 2 or more antennas are used. For larger rates, only 4 antennas are needed to bring the variance of the error much closer to the CRLB.

3.2 Rayleigh Amplitude Model

3.2.1 Maximum Likelihood Estimation

We derive a recursive algorithm for the estimate:

$$\hat{\lambda}^{[k+1]} = \frac{1}{A} \frac{\sum_{n=1}^{\infty} \frac{(\hat{\lambda}^{[k]} A)^n \exp(-\psi/n)}{n! n^{(L-1)}}}{\sum_{n=1}^{\infty} \frac{(\hat{\lambda}^{[k]} A)^n \exp(-\psi/n)}{n! n^L}} \quad (9)$$

The EM algorithm was numerically implemented for various values of λ (assumed known), starting with admissible initial estimate $\hat{\lambda}^{[0]} \geq 0$. The results after k iterations are shown in Fig. 5 for 4 antennas.

3.2.2 Performance of the Maximum Likelihood Estimator

Using Monte Carlo simulation of the power measurements, we estimate the bias, error variance, and the CRLB. The results are illustrated in Figs. 6 and 7. Figure 6 shows that the bias is reduced as the number of diversities increases. This follows from the fact that the ML estimator is consistent. We also note that as the rate increases, so does the variance of the Poisson process. This is evident in Fig. 6 since the statistical fluctuation in the estimate $E(\hat{\lambda})$ gets larger as the rate λ is increased, a fundamental Poisson property.

A comparison between the estimated error variance and the estimated CRLB is provided in Figure 7 for different numbers of diversities. For a fixed number of diversities, the variance of the error and the CRLB increase as the rate gets larger. As the number of diversities increases, the variance of the error and the CRLB decrease, and the variance of the error gets closer to the CRLB. Again, this is expected because the ML estimator is consistent.

For a large number of antennas ($L = 4$), the error variance and the CRLB get very close and the ML estimator becomes optimal in the sense that no other conceivable estimator having the same bias with the same data can perform better.

4. DISCUSSION

In this section, we provide a comparison between the performance of the ML estimators in the constant amplitude and Rayleigh models.

The performance of the ML estimator over regions where the rate λ not sufficiently large is better in the constant amplitude model than in the Rayleigh amplitude model. This can be seen by comparing how

close the error variance is to the CRLB in Fig. 4 versus Fig. 7, especially for the cases when $L = 2$ and 4.

Hence, the difference between the performances of the ML estimators for both models is notable when the rate λ is small. On the other hand, when the rate is sufficiently large, the performances of the estimators are quite comparable. This is justified by the fact that for large rates, the likelihood function in the constant amplitude model is very similar to the one in the Rayleigh model.

In the limit when the number of points N gets very large (fully developed model), it follows from the CLT that the likelihood function of the multi-diversity statistic ψ obeys a Gamma law \mathcal{GL}, λ . The statistic ψ is thus a complete sufficient statistic for the average scatterer density λ , and $\hat{\lambda} = \psi/L$ is the minimum variance unbiased estimator (MVUE) and the maximum likelihood estimate of the parameter λ .

Estimating the intensity of the point process quantifies the average received diffuse power and consequently the SINR. Using Eq. (1), the average channel capacity can also be estimated using a moment matching estimator type (in accordance with the law of large numbers) using the diversity measurements $\{\nu_{NI}\}$:

$$\hat{C} = B \sum_{l=1}^L \log_2 \left(1 + \frac{\nu_{NI}}{E(|n(t)|^2)} \right), \quad (10)$$

where $E(|n(t)|^2)$ is the mean-square of the interfering additive noise.

5. CONCLUSION AND SIGNIFICANCE

In this paper, we considered fading noise from a novel point of view: as a carrier of useful signal's power information. We presented estimation algorithms to the average received power, and consequently average received SINR, BER, and channel capacity using diffuse power measurements. The estimation schemes were based on a doubly stochastic filtered compound Poisson process and were applied to the particular models of constant and Rayleigh distributed amplitudes.

The structure and performance of these estimators differ significantly from that of estimation in additive noise and are a function of the particular point process parameters used to model the received fading power. We showed that the performance of the estimators improved as the number of diversity signals (or antennas) was increased. For 2 diversity and rates less than 20, the maximum likelihood estimator was optimal in the sense that the variance of the error is the smallest possible using any other conceivable estimate having the same bias with the same data. The maximum likelihood becomes optimal for all rates as the number of diversities is increased to 4 or more.

Since the developed estimation techniques are *optimal* and *computationally efficient*, they can serve as a powerful tool for accurate stochastic characterization of wireless channels leading to effective performance analysis, QoS guarantee, and link capacity analysis. Next generation WLAN and WPAN networks with SLAC channels can especially benefit from these results.

6. FUTURE WORK

For future work, there is the possibility of precomputing the EM algorithm on a quantized set of input statistics, that is, effectively vector-quantizing the input measurements and running the EM algorithm for each VQ quantization cell. This then reduces the computation of the estimate to a quantization and lookup-table problem. There is obviously an interesting trade-off here between quantizer rate or number of bits to represent a quantization cell and the estimator accuracy. Such a study is beyond the scope of this paper and constitutes a future direction of investigation.

Another possible future direction of research is to explicitly consider other models for the marks associated with each of the scattering centers [9], whose locations are in general assumed to be given by an inhomogeneous spatial Poisson process. Such analysis would extend our work to various fading environments such as mobile, polarized, and shadow fading.

REFERENCES

- [1] J. Anderson, "Antenna Arrays in Mobile Communications: Gain, Diversity, and Channel Capacity," *IEEE Antennas and Propagation Magazine*, vol. 42, pp. 12-16, April 2000.

- [2] T. Cover and J. Thomas, *The Elements of Information Theory*, John Wiley & Sons, New York, 1991.
- [3] N. Blaunstein and . Andersen, *Multipath Phenomena in Cellular Networks*, Artech House, MA, 2003.
- [4] R. Prasad and L. Munoz, *WLANs and WPANs Towards 4G Wireless*, Artech House, MA, 2003.
- [5] J. Winters, "Smart Antennas for Wireless Systems," *IEEE Personal Communications*, vol. 1, pp. 23-27, Feb. 1998.
- [6] D. Snyder and M. Miller, *Random Point Processes in Time and Space*, NY: Springer-Verlag, 2002.
- [7] M. Simon and M. Alouini, *Digital Communication over Fading Channels*, Wiley-Interscience, 2000.
- [8] J. Daba and M. Bell, "Statistics of the Scattering Cross Section of a Small Number of Random Scatterers," *IEEE Transactions on Antennas and Propagation*, August 1995.
- [9] J. Daba and M. Bell, "Statistical Distributions of Partially Developed Speckle Based on a Small Number of Constant Scatterers with Random Phase," *IEEE Geoscience & Remote Sensing Symp.*, Aug. 94.

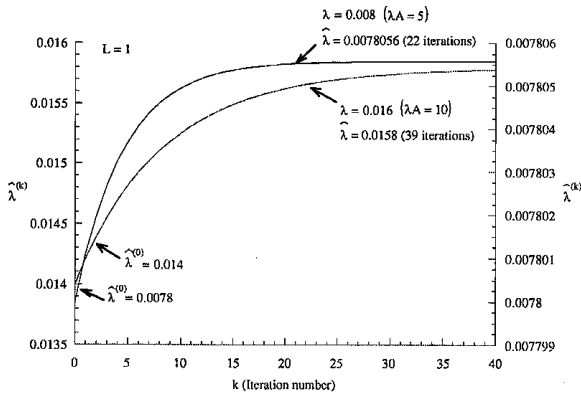


Fig. 1: Sequences of EM estimates for a single-diversity and various rates λA . (Constant amplitude model)

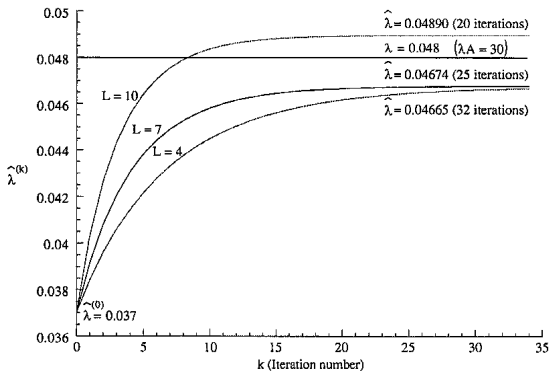


Fig. 2: Sequences of EM estimates for a fixed rate λ and different diversities. (Constant amplitude model)

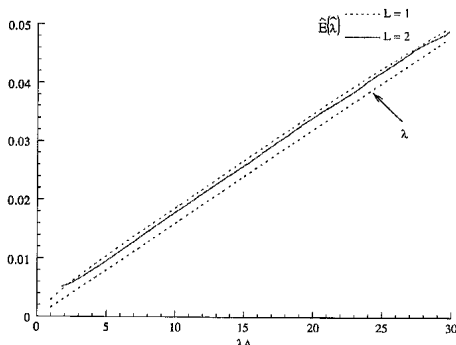


Fig. 3: Estimated bias of the ML estimator as a function of the rate λ for 1 and 2 diversities.

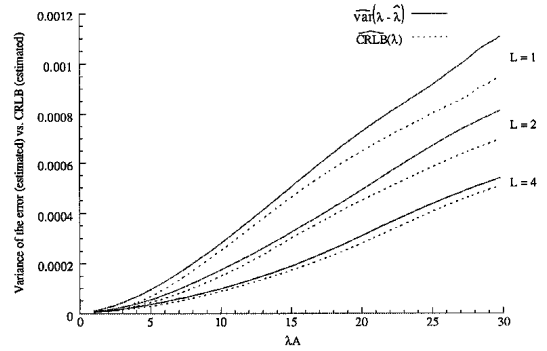


Fig. 4: Estimated variance of the error of the ML estimator compared to the estimated CRLB as a function of the rate λ . (Constant amplitude model)

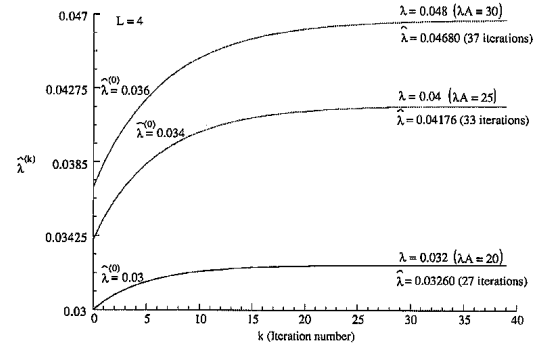


Fig. 5: Sequences of EM estimates for 4 diversities and different rates λ . (Rayleigh amplitude model)

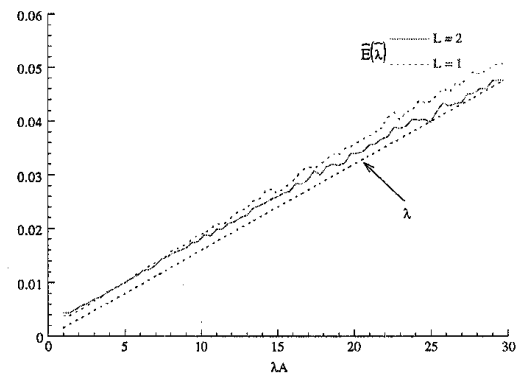


Fig. 6: Estimated bias of the ML estimator as a function of the rate λ for 1 and 2 diversities, using 3000 runs. (Rayleigh amplitude model)

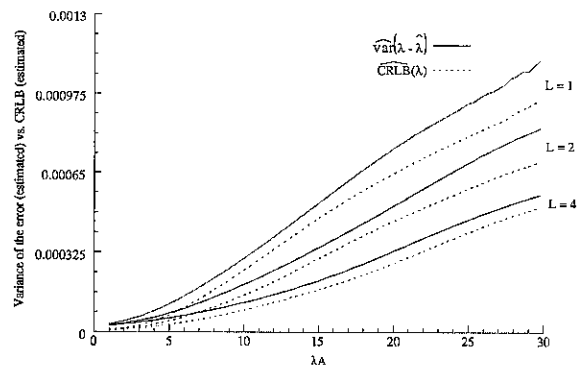


Fig. 7: Estimated error variance of the ML estimator (using 10000 runs) compared to the estimated CRLB as a function of the rate λ . (Rayleigh amplitude model)